FEBS Letters 588 (2014) 2154–2161

journal homepage: www.FEBSLetters.org

Human Tudor staphylococcal nuclease (Tudor-SN) protein modulates the kinetics of *AGTR1-3′UTR* granule formation

Xingjie Gao [a,b,c,d,1], Xuebin Shi [a,c,d,1], Xue Fu [a,b,c,d,1], Lin Ge [a,c,d], Yi Zhang [a,b,c,d], Chao Su [a,b,c,d], Xi Yang [e], Olli Silvennoinen [f], Zhi Yao [a,c,d], Jinyan He [a,c,d], Minxin Wei [g,*], Jie Yang [a,b,c,d,*]

[a] Department of Biochemistry and Molecular Biology, Department of Immunology, School of Basic Medical Sciences, Tianjin Medical University, Tianjin 300070, China
[b] Laboratory of Molecular Immunology, Research Center of Basic Medical Science, Tianjin Medical University, Tianjin 300070, China
[c] Tianjin Key Laboratory of Cellular and Molecular Immunology, Tianjin Medical University, Tianjin 300070, China
[d] Key Laboratory of Educational Ministry of China, Tianjin Medical University, Tianjin 300070, China
[e] Department of Immunology, University of Manitoba, 471 Apotex Centre, 750 McDermot Avenue, Winnipeg R3E 0T5, Canada
[f] Institute of Medical Technology, University of Tampere, Tampere University Hospital, Biokatu 8, FI-33014 Tampere, Finland
[g] Department of Cardiovascular Surgery, Tianjin Medical University General Hospital, Tianjin 300070, China

ARTICLE INFO

Article history:
Received 18 March 2014
Revised 17 April 2014
Accepted 25 April 2014
Available online 8 May 2014

Edited by Michael Ibba

Keywords:
Tudor-SN
Stress granules
AGTR1
3′UTR

ABSTRACT

Human Tudor staphylococcal nuclease (Tudor-SN) interacts with the G3BP protein and is recruited into stress granules (SGs), the main type of discrete RNA-containing cytoplasmic foci structure that is formed under stress conditions. Here, we further demonstrate that Tudor-SN binds and co-localizes with *AGTR1-3′UTR* (*3′-untranslated region of angiotensin II receptor, type 1* mRNA) into SG. Tudor-SN plays an important role in the assembly of *AGTR1-3′UTR* granules. Moreover, endogenous Tudor-SN knockdown can decrease the recovery kinetics of *AGTR1-3′UTR* granules. Collectively, our data indicate that Tudor-SN modulates the kinetics of *AGTR1-3′UTR* granule formation, which provides an additional biological role of Tudor-SN in RNA metabolism during stress.

1. Introduction

Stress granules (SG) are a type of cytoplasmic RNA foci that aggregate in response to environmental stress stimuli, such as heat shock, oxidative stress, or viral infection, and play diverse roles in the regulation of mRNA translation, storage, stability, and decay [1–6]. SGs contain arrested preinitiation complexes, untranslated mRNAs, RNA-binding proteins, and other stress-related proteins, such as Ras-GAP SH3 domain-binding protein (G3BP) [7,8], TIA-1-related protein (TIAR) [7,9], and Tudor-SN [10–12]. SGs provide a temporal reservoir for mRNAs released from polysomes during stress, which also allows the resumption of translation after the stress-inducing conditions have subsided. This process is dependent on a set of RNA-binding proteins [1–7]. The study on the roles of RNA binding proteins in the stress-induced remodeling of mRNP (messenger ribonucleoprotein) complexes is an important issue.

Tudor-SN protein, also known as SND1 (staphylococcal nuclease domain containing 1) or p100, is evolutionarily conserved in humans [13–19], animals [20–22], and plants [23–25]. Human Tudor-SN is characterized by four N-terminal tandem repeats of the staphylococcal nuclease-like domain (SN) and a C-terminal TSN (Tudor-SN5) domain [13,14]. Tudor-SN plays several distinct roles by binding different protein partners or RNA substrates. For example, Tudor-SN functions as a transcriptional co-activator through an interaction between its SN domain and basal transcription machinery, such as CREB-binding protein (CBP) and RNA polymerase II [15,16], while taking part in pre-mRNA splicing through the binding of the TSN domain with symmetrical dimethylarginine-modified Sm core proteins of the spliceosome [17,18]. Our previous study indicated that Tudor-SN efficiently associated and co-localized with G3BP in SGs via the SN domain [10]. Accumulating evidence has revealed that Tudor-SN is a type of RNA-binding protein and that this function is mainly mediated through its SN domain [14,19,24–27]. It is interesting to study the role of Tudor-SN in RNA metabolism within SGs during stress. The SN domain of Tudor-SN was reported to interact with 3′UTR (3′-untranslated region) of *AGTR1* (*angiotensin II receptor, type 1*) mRNA under normal conditions [19]. Here, we further demonstrate

* Corresponding authors. Address: Department of Biochemistry and Molecular Biology, Department of Immunology, School of Basic Medical Sciences, Tianjin Medical University, Tianjin 300070, China (J. Yang).
E-mail addresses: minxinw@126.com (M. Wei), yangj@tijmu.edu.cn (J. Yang).
[1] These authors contributed equally to this work.

http://dx.doi.org/10.1016/j.febslet.2014.04.045
0014-5793/

that Tudor-SN binds and co-localizes with *AGTR1-3′UTR* in SG under stress conditions, which leads us to study the potential post-transcriptional regulatory mechanism of Tudor-SN on *AGTR1* mRNA-containing SG formation.

AGTR1 protein, a member of G protein-coupled receptor family, is involved in the physiological actions of Angiotensin II (Ang II) [28,29]. The expression of AGTR1 can be greatly affected by post-transcriptional regulation of *AGTR1* mRNA following treatment of cells with estrogen, Ang II, H_2O_2, or insulin [30–34]. For example, insulin up-regulates AGTR1 expression by stabilizing *AGTR1* mRNA in a 3′UTR dependent manner [34]. In the present study, we demonstrate that Tudor-SN is important for *AGTR1-3′UTR* granule aggregation, and the knockdown of endogenous Tudor-SN decreases the SG recovery kinetics.

2. Materials and methods

2.1. Cell culture, plasmids and transfection

HeLa cells were cultured as described previously [16]. Tudor-SN siRNA was generated as previously reported [15,18]. The plasmid encoding RFP-epitope-tagged Tudor-SN (RFP-Tudor-SN) was generated as described previously [10]. The pGenesil-DsRed-Tudor-SN-shRNA and pGenesil-DsRed-scramble-shRNA plasmids were constructed by Wuhan Cell Marker Biotechnology (China). The GFP-MS2 system was constructed as follows: pCR4-24×MS2SL-stable, pMS2-GFP plasmid encoding GFP-MS2 were a kind gift from Dr. Robert H. Singer (Albert Einstein College of Medicine, Bronx, NY, USA) (Addgene plasmid). To generate pT7-AGTR1-3′UTR, the *AGTR1-3′UTR* (1430–1993 bp) fragment was amplified by polymerase chain reaction (PCR) with the primers EcoRI-forward (5′-CGAATTCTCCACCAAGAAGCCTGCACCATG-3′) and BamHI-reverse (5′-CCGGATCCGCAACTTGACGACTACTGCTTA-3′), using AGTR1 total cDNA transcript (OriGene) as a template. This fragment was ligated into empty pSG5 vector containing the T7 bacteriophage promoter via EcoRI and BamHI enzymes. 24×MS2 stem loop repeats were cut from pCR4-24×MS2SL-stable plasmid and subsequently ligated into pT7-AGTR1-3′UTR or pSG5 using BglII and BamHI enzymes to construct the pT7-AGTR1-3′UTR-24×MS2 or pT7-24×MS2 plasmids. All PCR products were sequenced.

siRNA and plasmids were transfected using Lipofectamine 2000 (Invitrogen), according to the manufacturer's protocol. GFP-MS2 system plasmids were transfected using Neofect™ DNA transfection reagent (China).

2.2. Fast protein liquid chromatography (FPLC) assay

Different cellular fractions were prepared as described previously [35]. Total cell lysates from HeLa cells treated with 0.5 mM arsenite sodium for 1 h were harvested with Nonidet P-40 lysis buffer that was supplemented with protease inhibitor cocktail (Roche Diagnostics) and RiboLock ribonuclease inhibitor (MBI) at 4 °C. Approximately 10 mg of protein was concentrated to 500 μl using an Ultrafree centrifugal filter apparatus (10 kDa nominal molecular mass limit, Millipore) and then applied to a Superose 6 size exclusion column (850 mm × 20 mm, GE Healthcare). The column was eluted at a flow rate of 0.5 ml/min. Each 500 μl fraction was collected and divided into two portions equally. One portion was used to perform Western blotting assay with rabbit anti-Tudor-SN (Abcam), anti-Tubulin (Abcam), and anti-TIAR (Cell Signaling Technology) antibodies, and the other was used for reverse transcription-PCR to analyze the distribution of *AGTR1* and *GAPDH* mRNA. The *AGTR1* primers sequences were 5′-TCCACCAAGAAGCCTGCACCA-3′ (forward); 5′-TGGGACCAGTGC AGCACCTT-3′ (reverse), which were also used in the RIP and RNA FISH assays. The primer sequences of *GAPDH* were reported previously [18].

2.3. RNA-binding protein immunoprecipitation (RIP) assay

RIP Assay was performed as reported previously [18]. Total cell lysates from HeLa cells were incubated with rabbit anti-Tudor-SN antibody (Santa Cruz Biotechnology) or rabbit anti-IgG (Santa Cruz Biotechnology) conjugated with Protein G Dynabeads (Invitrogen) at 4 °C overnight with head-over-tail rotation. The precipitated *AGTR1* mRNAs were detected by the reverse transcription-PCR assay, and the enriched Tudor-SN was confirmed by Western blotting assay using rabbit anti-Tudor-SN antibody.

2.4. Immunofluorescence (IF) and live-cell imaging assays

The IF and live-cell imaging assays were performed as described previously [10]. Briefly, cells were fixed, permeabilized, and then incubated with goat anti-Tudor-SN (Santa Cruz Biotechnology) at 4 °C overnight. After washing, cells were incubated with donkey anti-goat IgG (TR) antibody (Abcam) or Alexa Fluor 488-coupled donkey anti-rabbit IgG antibody (1:800 dilution) at 4 °C overnight. Images were collected using an Olympus FV1000 confocal microscope. The OLYMPUS IX81-CSU live cell system was used for live-cell imaging.

2.5. RNA fluorescence in situ hybridization (RNA FISH) assay

HeLa cells were fixed and permeabilized as described previously [10]. After denaturation in 25% formamide at 95 °C for 3 min and placement on ice for 3 min, 6 ng/μl biotinylated *AGTR1* probe was incubated with the cells in a humidified dark chamber at 40 °C overnight. The cells were then sequentially washed with 25% formamide diluted in 0.5×SSC for 15 min, 2×SSC for 10 min, and 4×SSC for 10 min. The hybridization signal was detected using 2.5 μg/ml FITC-avidin (Invitrogen) in 2×SSC containing 0.2% bovine serum albumin and 0.01% Tween 20. For biotinylated *AGTR1* probe, the *AGTR1-3′UTR* (1430–2135 bp) fragment was amplified by PCR using AGTR1 total cDNA transcript (OriGene) as a template. The PCR product was purified with Gel/PCR Extraction Kit (Biomiga) and biotinylated using a Biotin-Nick Translation Kit (Roche Diagnostics).

2.6. Fluorescence recovery after photobleaching (FRAP) experiment

HeLa cells were cultured in 20 mm glass-bottomed Petri dishes (NEST Biotechnology) and co-transfected with ATGR1-3′UTR-MS2-GFP system plasmids and Tudor-SN shRNA or scramble shRNA. Twenty-four hours after transfection, cells were treated with 0.5 mM sodium arsenite (Sigma) for 30 min and kept in a phenol red-free medium. FRAP experiments were carried out using an Olympus FV1000 confocal microscope. Each granule region of interest (ROI) was randomly selected in a square area, and bleaching was performed with the 405 nm wavelength operating at 50% laser power and 10 μs/pixel scan speed for 2.5 s. Fluorescence recovery was monitored by the FRAP analysis tool (Olympus) at a low laser intensity every 5 s over a 200-sec period.

2.7. Granule quantification and statistical analysis

All experiments were repeated at least three times. Approximately 100 cells per experiment were scored randomly. The number and size of granules in the cells were measured using a

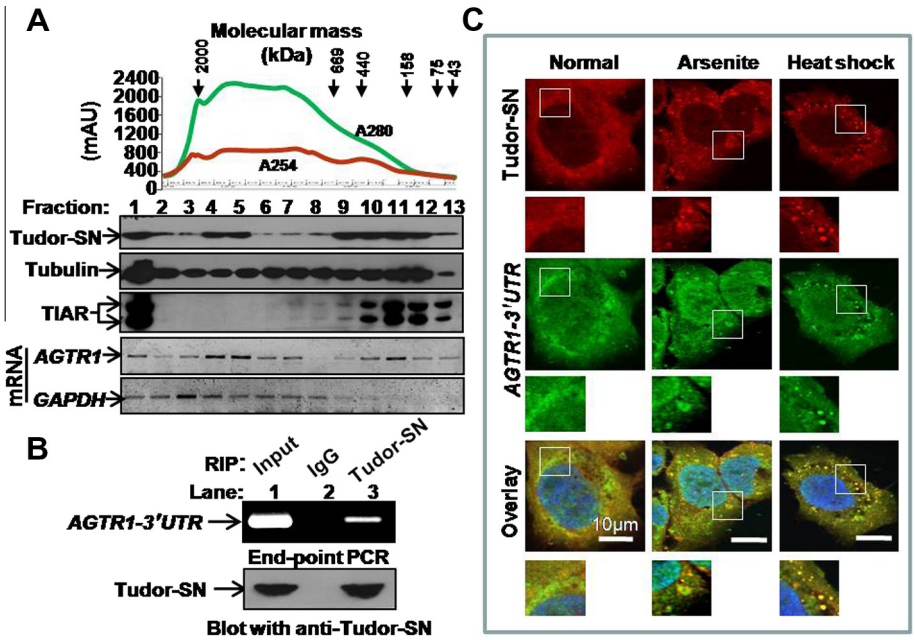

Fig. 1. Tudor-SN binds and co-localizes with *AGTR1-3′UTR* in SG under stress condition. (A) Analysis of the Tudor-SN-*AGTR1-3′UTR* complex profile using FPLC. Total cell lysates from HeLa cells were fractionated on Superose 6 size exclusion columns. Every 500 μl chromatographic fraction was divided into two portions equally. Then, 250 μl was subjected to SDS–PAGE and Western blotting with antibodies, including anti-Tudor-SN, anti-Tubulin, and anti-TIAR. The extracted mRNA from the other 250 μl was reverse-transcribed to cDNA with oligo$(dT)_{18}$ primers and then analyzed by reverse transcription-PCR assay using primers specific for the *AGTR1* and *GAPDH* mRNA. The chromatographic profile with the elution positions of calibrating proteins of known molecular masses (kDa) and absorbance profile at 280 nm and 254 nm were shown on top. Five percent of the total cell lysate was included as input loading in fraction 1. (B) Tudor-SN binds *AGTR1-3′UTR* in vivo. RIP assays were performed on HeLa cells with Dynabeads-bound rabbit anti-Tudor-SN and rabbit IgG antibody (negative control), respectively, followed by the reverse transcription-PCR of *AGTR1-3′UTR* (upper panel). The enriched Tudor-SN was confirmed by the Western blotting assay using rabbit anti-Tudor-SN antibody (lower panel). Five percent of the total cell lysate was included as input. (C) Tudor-SN co-localizes with endogenous *AGTR1-3′UTR* in SG. HeLa cells were treated with sodium arsenite (0.5 mM), heat shock (45 °C) for 45 min or control conditions (Normal). RNA-FISH assay was performed with 6 ng/μl biotinylated *AGTR1* probe and 2.5 μg/ml FITC-avidin, as described in the Section 2 section. Scale bars, 10 μm.

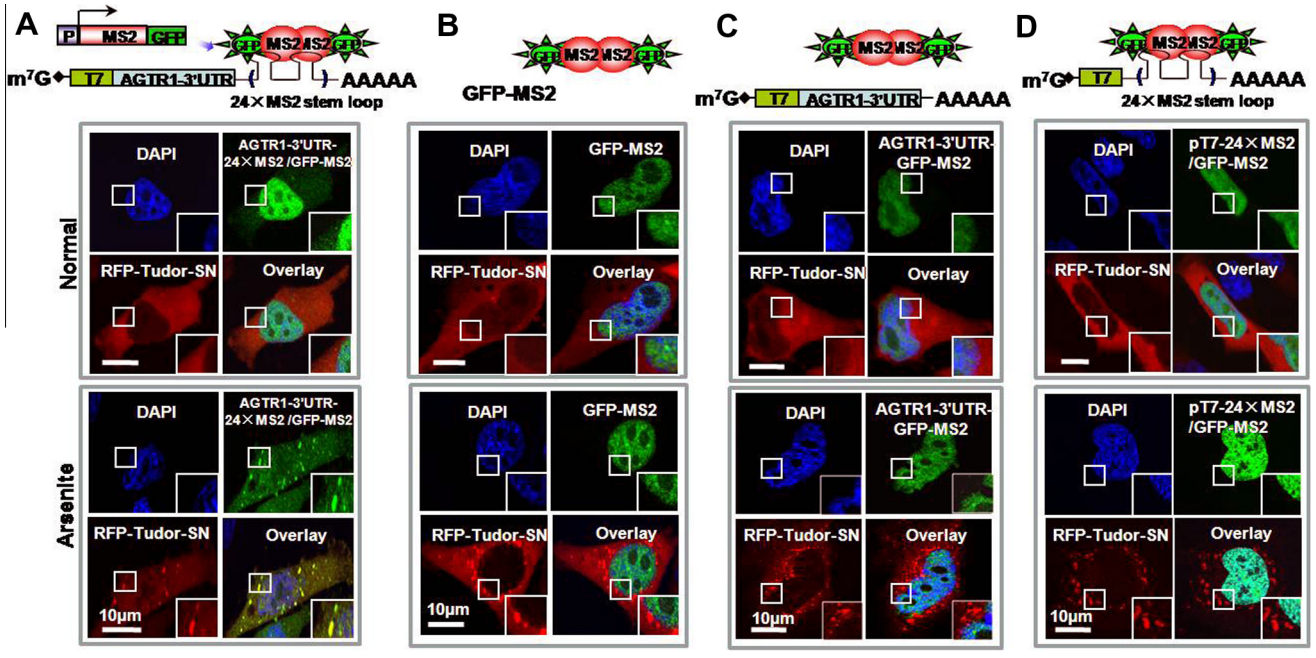

Fig. 2. Tudor-SN co-localizes with *AGTR1-3′UTR* granules using the GFP-MS2 labeling system. HeLa cells grown on glass cover slips were transfected with RFP-Tudor-SN plasmid together with GFP-MS2 labeling system plasmids, as indicated, and either treated with 0.5 mM sodium arsenite for 1 h or left untreated (Normal). Confocal microscopy analysis was then performed. The schematic diagram of the GFP-MS2 labeling system was shown on the top. Scale bars, 10 μm.

blind counting method with the Image J software (National Institutes of Health). The data are presented as the means ± S.E. (Standard Error) or box-plots (granule size analysis) and compared using Independent-Sample Student's *T* Tests with the SPSS 16.0 software. *P* values less than 0.05 were considered statistically significant.

3. Results

3.1. Tudor-SN binds and co-localizes with AGTR1-3′UTR in SG under stress conditions

Previously, it was shown that Tudor-SN binds the 3′UTR of *AGTR1* mRNA under normal conditions [19]. To gain insight into the association between Tudor-SN and *AGTR1-3′UTR* under stress conditions, protein-RNA fractionation experiments were performed through size exclusion approach by FPLC assay. Total cell lysates from HeLa cells were fractionated by a Superose 6 gel filtration column. As shown in Fig. 1A, the elution pattern of Tudor-SN in chromatographic fractions showed a major peak at approximately 158-669 kDa and a minor peak at higher molecular masses (slightly below 2000 kDa). Moreover, the major peak largely overlapped with that of the SG protein components, including TIAR and Tudor-SN. Tubulin protein was distributed throughout the chromatographic fractions. Furthermore, both peaks of Tudor-SN co-eluted with *AGTR1* mRNA, but not *GAPDH* mRNA. The result in Fig. S1 showed that Tudor-SN protein fails to colocalize with the PB-specific protein DCP1a, confirming that Tudor-SN is one type of SG-specific protein, in agreement with the data of Weissbach, R. [7]. These findings suggest that Tudor-SN-*AGTR1* mRNA binding is associated with SG biogenesis.

We then performed RIP assays to confirm the interaction between Tudor-SN and *AGTR1-3′UTR* under stress conditions. As shown in Fig. 1B, the anti-Tudor-SN antibody could efficiently precipitate with the *AGTR1-3′UTR* (lane 3), but not the control anti-IgG antibody (lane 2), which indicated that Tudor-SN readily interacts with the 3′UTR of *AGTR1* in vivo under stress. Furthermore, we also detected the in vivo colocalization of Tudor-SN and *AGTR1-3′UTR* by RNA FISH with a FITC-labeled *AGTR1* probe and in an IF assay using anti-Tudor-SN antibody. As shown in Fig. 1C, both endogenous Tudor-SN protein and *AGTR1-3′UTR* mRNA predominantly accumulated in SG under stress. The above findings indicate that Tudor-SN associates with and targets *AGTR1* mRNA in the SG structure.

3.2. Tudor-SN co-localizes with AGTR1-3′UTR granules using a GFP-MS2 labeling system

To monitor the aggregation of *AGTR1-3′UTR* granules in living cells, we labeled the *AGTR1-3′UTR* using the GFP-MS2 labeling system, which is useful for visualizing the real-time motion of single mRNA molecules [36]. As shown in the schematic diagram of Fig. 2, we tethered the targeting *AGTR1-3′UTR* fragment with 24 copies of the bacteriophage MS2 stem loops to generate the pT7-AGTR1-3′UTR-24×MS2 plasmid, which can bind multiple

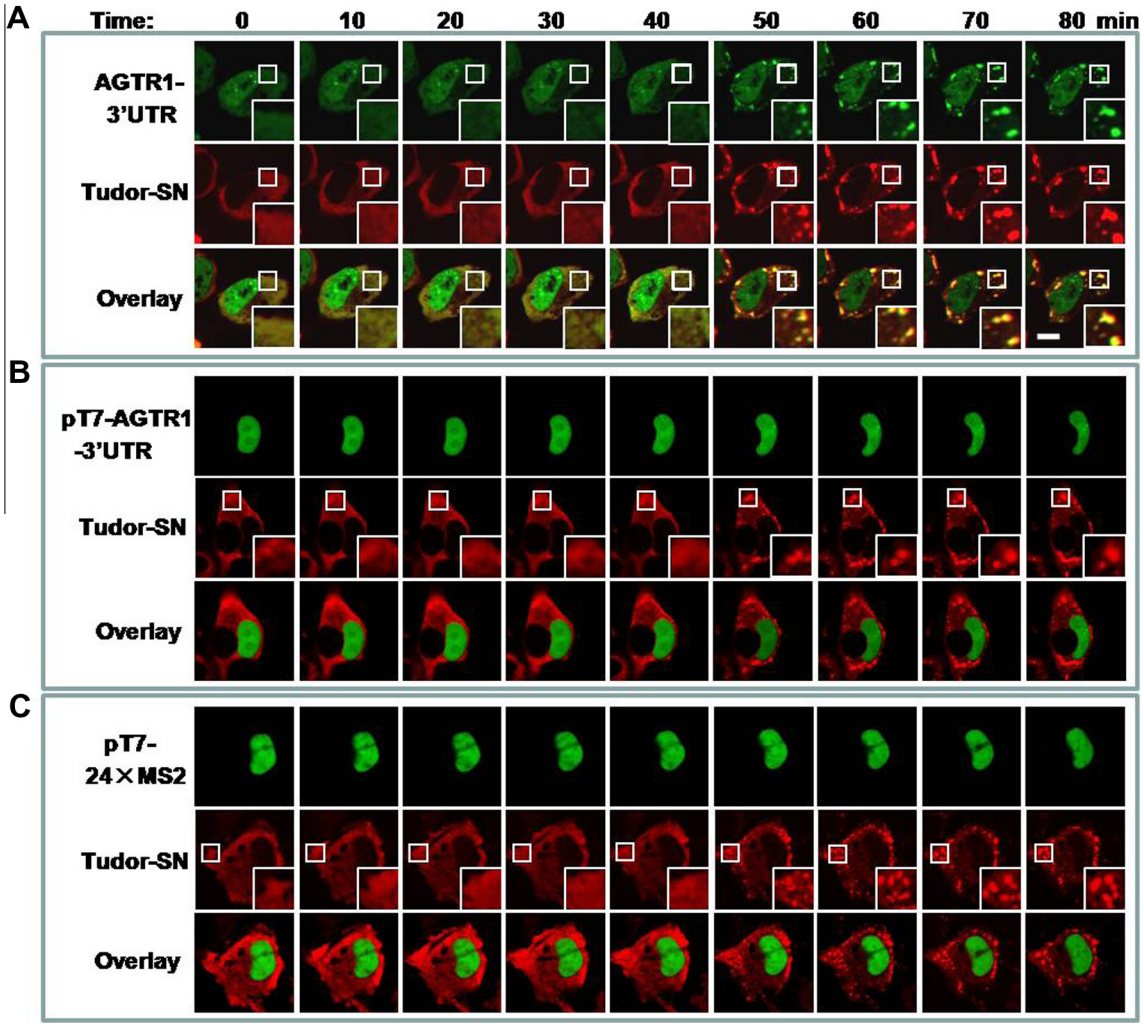

Fig. 3. Kinetic experiments on the co-localization of Tudor-SN and *AGTR1-3′UTR* granules in live cells during stress. The movement of Tudor-SN granules was correlated with *AGTR1-3′UTR* in live cells. HeLa cells were transfected with the RFP-Tudor-SN and GFP-MS2 labeling system plasmids, as indicated, and monitored using OLYMPUS IX81-CSU live cell system in the presence of 0.1 mM sodium arsenite. Scale bars, 10 μm.

GFP-tagged bacteriophage MS2 coat proteins (GFP-MS2) with a strong affinity, encoded by the pMS2-GFP plasmid. Hence, the localization and movement of *AGTR1-3′UTR* in live cells can be tracked. pT7-AGTR1-3′UTR-24×MS2, pMS2-GFP and RFP-tagged Tudor-SN plasmids were transiently co-transfected into HeLa cells. As expected, the *AGTR1-3′UTR* fragment (green) co-localized with Tudor-SN (red) in arsenite-treated cells (Fig. 2A). In contrast, under normal conditions, a weak signal was detected in the cytoplasm and a strong signal was detected in the nucleus, due to the NLS (nuclear localization signal) element harbored in the pMS2-GFP plasmid. To verify the specific recognition of Tudor-SN with the *AGTR1-3′UTR* in vivo, HeLa cells were co-transfected with pMS2-GFP plasmid and RFP-tagged Tudor-SN plasmid, together with pT7-AGTR1-3′UTR or pT7-24×MS2. As shown in Fig. 2B–D, neither lacking *AGTR1-3′UTR* reporter nor lacking the 24×MS2 stem loop repeats exhibits cytoplasmic foci, but the foci instead remain localized to the nucleus. Tudor-SN specifically interacts with the *AGTR1-3′UTR*, but not the poly(A) tail, because Tudor-SN did not colocalize with pT7-24×MS2, which only contains the poly(A) tail (Fig. 2D). In addition, the data in Figs. S2 and S3 indicate that *AGTR1-3′UTR* is co-localized with another SG-specific protein, TIAR, but not the PB-specific protein DCP1a under stress conditions, confirming that these *AGTR1-3′UTR* granules are SG-specific, but not PB-specific. Live-cell imaging revealed the dynamic association of RFP-tagged Tudor-SN protein and GFP-tethered reporter *AGTR1-3′UTR* granules during cellular oxidative stress, but no interaction was observed with control plasmids (Fig. 3). These data indicate that the SG recruitment of the *AGTR1* transcript is accompanied by the formation of Tudor-SN granules.

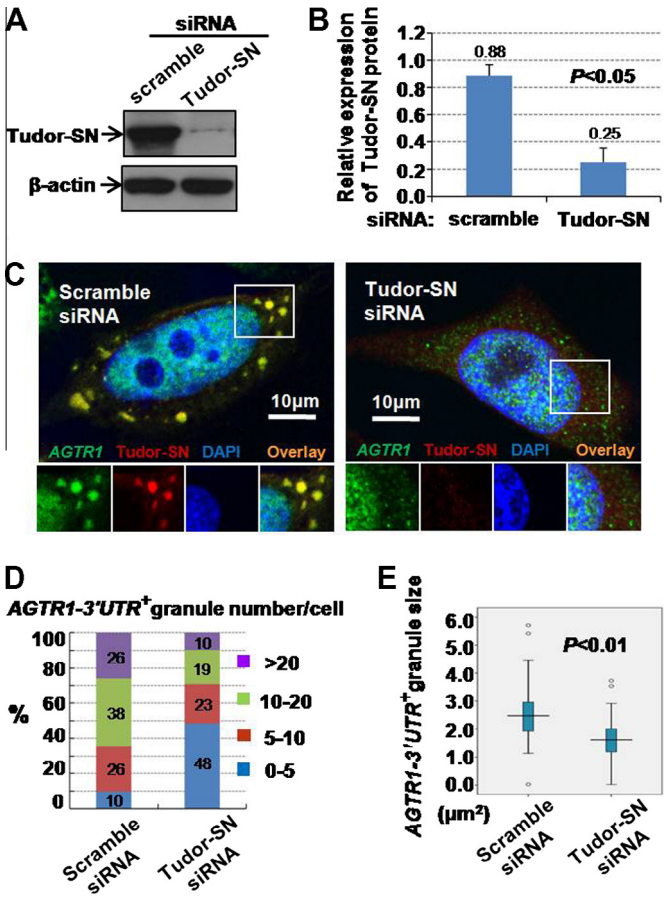

Fig. 4. The knockdown of Tudor-SN impairs the formation of GFP-tagged *AGTR1-3′UTR* granules. (A) HeLa cells were transfected with the Tudor-SN siRNA or scramble siRNA as control. After 48 h, the total cell lysates from transfected cells were subjected to SDS–PAGE and then blotted with anti-Tudor-SN (upper panel) or anti-β-actin antibody as a control (lower panel). (B) Band density was digitized using the TotalLab software, and the expression level of Tudor-SN was normalized against the β-actin protein. An independent-sample Student's *T* Test was performed, and significant differences are indicated as follows: $P < 0.05$. (C) HeLa cells were co-transfected with pT7-AGTR1-3′UTR-24×MS2/pMS2-GFP, Tudor-SN siRNA, or scramble siRNA as control. Image data were collected by confocal microscopy. Scale bars, 10 μm. (D) The granule size was analyzed and displayed as a box-plot. Independent-Samples Student's *T* Test was performed using SPSS16.0. The significant difference was indicated: $P < 0.01$. (E) The number of *AGTR1* granules per cell was also measured by Image J. The cells were divided into four categories of granule number per cell: 0–5, 5–10, 10–20 and >20.

3.3. Tudor-SN plays an important role in the assembly of AGTR1-3′UTR granules

Nascent SGs are small and then progressively fuse into larger foci [9]. Dynamic packaging of the cellular mRNA transcript by stress-related proteins is essential for the remodeling and recruitment of cytoplasmic mRNP complexes into SGs [1–6]. We previously demonstrated that the knockdown of Tudor-SN does not inhibit the formation of SG but instead retards the aggregation of small SGs into large SGs [10]. Tudor-SN is likely to be important for the assembly of *AGTR1-3′UTR*-containing SGs. We analyzed the number and size of *AGTR1-3′UTR* granules when the endogenous Tudor-SN protein was knocked down by siRNA treatment. As shown in Fig. 4A and B, the transfection of Tudor-SN siRNA significantly reduced the expression of Tudor-SN protein by approximately 70% ($P < 0.05$), compared with the scramble siRNA, but had no effect on the abundance of β-actin. Moreover, the knockdown of Tudor-SN significantly reduced the size of *AGTR1-3′UTR* granules in single cells (Fig. 4C–E, $P < 0.01$), while the proportion of cells containing >20 foci was also decreased (Fig. 4D, from 26% to 10%), suggesting that the knockdown of Tudor-SN hindered the emergence of *AGTR1-3′UTR* granules and led to a decrease in both the number and size of *AGTR1-3′UTR* granules. These data indicated that Tudor-SN is essential for SG recruitment of target *AGTR1* mRNA.

3.4. Tudor-SN affects the recovery kinetics of SGs

SGs are proposed to be the site where the local concentration of proteins and mRNAs is increased in response to environmental stress [1,6,7]. SGs are not stable structures that often exchange dynamically with the surrounding cytosol. Different SG components show different aggregation kinetics [7,37–39]. To quantitatively analyze the role of Tudor-SN in the association/dissociation dynamic properties of *AGTR1-3′UTR* granules in living cells under stress, we performed the FRAP assay, which has frequently been utilized to detect the recovery kinetics of fluorescent protein labeled components [7,38]. Because the combination of the MS2-GFP labeling system and the FRAP assay can be used to analyze the kinetics of targeting RNAs [39], we photo-bleached the nascent *AGTR1-3′UTR* labeled with MS2-GFP to analyze its exchange kinetic in HeLa cells with Tudor-SN knockdown. HeLa cells were transfected with pGenesil-DsRed-Tudor-SN-shRNA plasmid or pGenesil-DsRed-scramble-shRNA as the negative control, and Western blot and IF assays were then performed. The transfection efficiency of shRNA was determined by the expression of DsRed. The Western blot results (Fig. 5A and B) showed that the level of endogenous Tudor-SN protein but not β-actin protein was significantly reduced (upper panel) by the Tudor-SN shRNA treatment (lower panel) compared with the scramble shRNA group. Moreover, as shown in Fig. 5C, the IF signal (red) from the Tudor-SN protein was significantly reduced with Tudor-SN shRNA in the DsRed-positive cell (green), but not with scramble shRNA. Next, an analysis of the aggregation kinetics of *AGTR1-3′UTR* granules was performed using the FRAP assay when Tudor-SN was knocked down. HeLa cells

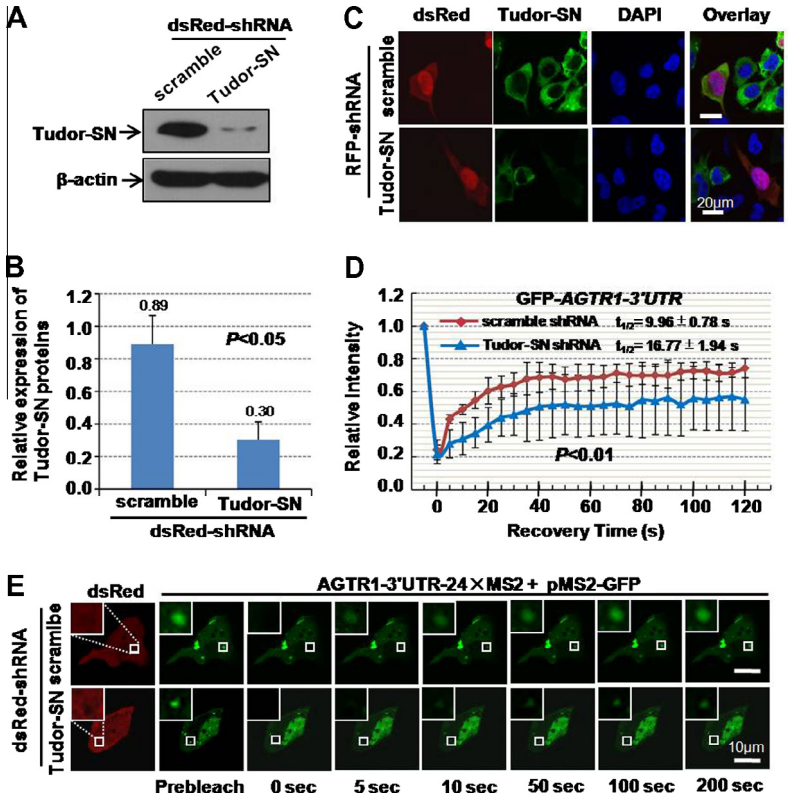

Fig. 5. Tudor-SN is important for *AGTR1-3′UTR* granule aggregation kinetics. FRAP analysis of GFP-tagged *AGTR1-3′UTR* with endogenous Tudor-SN was sufficiently down-regulated with RNA interference. (A) HeLa cells were transfected with the pGenesil-DsRed-Tudor-SN-shRNA plasmid (Tudor-SN shRNA) or the pGenesil-DsRed-scramble-shRNA plasmid (scramble shRNA) as the negative control. Total cell lysates from Tudor-SN shRNA- or scramble shRNA-treated HeLa cells were subjected to SDS–PAGE and then blotted with anti-Tudor-SN (upper panel) or anti-β-actin antibody as a control (lower panel). (B) Band density was digitized using the TotalLab software, and the expression level of Tudor-SN was normalized against β-actin. An independent-sample Student's *T* Test was performed, and significant differences are indicated as follows: $P < 0.05$. (C) Transfected cells were fixed and stained with rabbit anti-Tudor-SN antibody and Alexa Fluor 488-coupled donkey anti-rabbit IgG antibody. Confocal microscopy analysis was then performed. Scale bars, 10 μm. (D) HeLa cells were co-transfected with Tudor-SN shRNA, scramble shRNA, and ATGR1-3′UTR-MS2-GFP system plasmid, as indicated. After treatment with 0.5 mM sodium arsenite for 0.5 h, the FRAP assay was performed. The fluorescence signals from selected granules in DsRed-positive cells were irradiated with 50% power of the 405 nm laser, and recovery was recorded for 200 s. An independent-sample Student's *T* Test was performed, and significant differences are indicated as follows: $P < 0.01$. Scale bars, 10 μm. (E) Imaging data of FRAP analysis is shown.

were co-transfected with the ATGR1-3′UTR-MS2-GFP system plasmid together with Tudor-SN shRNA or scramble shRNA as a control and then treated with 0.5 mM sodium arsenite. Individual regions containing GFP-tagged *ATGR1-3′UTR* granules in the DsRed-positive cell were photobleached with a high-power laser. Remarkably, as shown in Fig. 5C and D, when Tudor-SN was knocked down, *AGTR1-3′UTR* demonstrated a slower recovery rate ($t_{1/2}$ = 16.77 ± 1.94 s) and less complete recovery (~56.8%) compared with the control group ($t_{1/2}$ = 9.96 ± 0.78 s, ~74.2% recovery) (Fig. 5D, $P < 0.01$), suggesting that Tudor-SN is necessary for the efficient cytoplasmic movement of exogenous *AGTR1-3′UTR* under stress conditions. In addition, as shown in Fig. S4, the knockdown of Tudor-SN fails to induce the aggregation of *AGTR1-3′UTR* under normal conditions, confirming that the role of Tudor-SN on *AGTR1-3′UTR* granule aggregation is dependent on an environmental stress. These quantitative kinetic data provide insights that Tudor-SN serves as an indispensable component to facilitate SG aggregation by interacting with SG-related mRNPs and modulating their kinetic nature under environmental stress.

4. Discussion

The posttranscriptional regulation of gene expression in eukaryotes involves several regulatory processes, such as mRNA nucleo-cytoplasmic export, cellular localization, translation regulation, and mRNA turnover, and often requires the interaction between RNA-binding proteins and conserved structural elements located in the 3′UTR of the mRNA molecule [40]. Several connections between Tudor-SN and 3′UTRs have been reported: (1) Tudor-SN in rice binds the 3′UTR of prolamine RNAs and is involved in RNA transport and localization in rice endosperm during rice seed development [24,25]. (2) Human Tudor-SN also interacts with the 3′UTR of the DENV (dengue virus) genome and is involved in virus replication [26]. (3) Tudor-SN binds SG-associated AGO2 protein and has been identified as a core component of RISC, which targets the 3′UTR of mRNA substrates [41]. These data favor the idea that 3′UTR binding is likely to be a type of approach for multifunctional Tudor-SN to modulate the cytoplasmic fate of specific mRNAs. Here, we present evidence that Tudor-SN binds and co-localizes with *AGTR1-3′UTR* in SG under stress conditions. Tudor-SN is also required for the efficient aggregation and recovery kinetics of *AGTR1-3′UTR* granules. These data indicate that Tudor-SN is likely to act as a key positive regulator for the recruitment of specific bound mRNA cargoes into insoluble SGs under stress and to modulate the increased flow of *AGTR1* mRNA that accompanies stress.

As the RNA-binding protein, Tudor-SN promotes the stabilization of certain mRNAs during stress. For example, Tudor-SN in Arabidopsis stabilizes the level of stress-responsive mRNAs encoding secreted proteins [23]. Tudor-SN enhances the expression of *AGTR1* by decreasing the rate of mRNA decay in non-stressed cells, However, Tudor-SN does not mediate the posttranscriptional regulation of *AGTR1* mRNA in response to atorvastatin, estrogen, insulin, or Ang II [19]. Although GAPDH was reported to increase

AGTR1 expression via the binding of *AGTR1-3′UTR* in response to H_2O_2 [31], we still lack evidence that human Tudor-SN modulates the retention or stability of *AGTR1-3′UTR* mRNA in SG structures during stress. In addition, *AGTR1-3′UTR* binds several other RNA-binding proteins as well, including calreticulin [30], AUF1 [32], GAPDH [31], and HuR [33,34]. Interestingly, HuR and calreticulin were confirmed to be SG components [42,43]. We also observed the binding of Tudor-SN and HuR/calreticulin (data not shown), suggesting that the post-transcriptional regulatory process of *AGTR1* mRNA might be dependent on the existence of the SG-associated protein complex containing Tudor-SN, HuR, and calreticulin or binding with the 3′UTR.

PB (Processing Body), another stress-associated cytoplasmic foci structure, contains microRNA (miRNA)-mediated RNA interference (RNAi) effectors and mRNA decapping machinery, which is involved in mRNA repression and degradation [3–7]. SG and PB share some common components and exhibit intricate connections on mRNA metabolism [3–7,44]. Translationally inactive mRNA within the SG can be delivered to PB for degradation [6,7,44]. Regarding *AGTR1*, we fail to observe the localization of *AGTR1* in the PB structure. However, we still cannot rule out the possibility of *AGTR1* degradation in the PB due to the limit of treatment time or drug concentration.

The AGTR1 protein is recognized by Ang II, a peptide hormone, and plays a pathophysiological role in atherosclerosis, hypertension, cardiac hypertrophy, kidney injury, and heart failure [28,29,45,46]. It was reported that the expression of Tudor-SN in rats is increased in response to H_2O_2-induced oxidative stress [21] or high glucose treatment [22]. The up-regulation of Tudor-SN in rats under hyperglycemic conditions leads to an increased level of AGTR1 protein expression and is involved in the modulation of glomerular injury [22]. Very recently, we demonstrated that Tudor-SN is essential for the adipogenesis [47]. It is possible that Tudor-SN functions in the pathophysiology of glucolipid metabolism-related diseases, such as atherosclerosis, by modulating the mobility or aggregation kinetics of AGTR1-containing SG under high glucose stress conditions, which merits further study.

Acknowledgments

We thank Xin Song, Xiaoyong Shen, Zhe Liu, Haifang Yin, and Rongxin Zhang (Research Center of Basic Medical) for excellent technical assistance and helpful comments. This work was supported by Grants from the National Science Foundation for Distinguished Young Scholars of China (31125012), NSFC (21305103, 31100967, 31170830 and 31370749), Program for Innovative Research team of Ministry of Education (IRT13085) and China Postdoctoral Science Foundation funded project (2013T60258).

Appendix A. Supplementary data

Supplementary data associated with this article can be found, in the online version, at http://dx.doi.org/10.1016/j.febslet.2014.04.045.

References

[1] Buchan, J.R. and Parker, R. (2009) Eukaryotic stress granules: the ins and outs of translation. Mol. Cell. 36, 932–941.
[2] Anderson, P. and Kedersha, N. (2009) RNA granules: post-transcriptional and epigenetic modulators of gene expression. Nat. Rev. Mol. Cell Biol. 10, 430–436.
[3] Kedersha, N. and Anderson, P. (2009) Regulation of translation by stress granules and processing bodies. Prog. Mol. Biol. Transl. Sci. 90, 155–185.
[4] Thomas, M.G., Loschi, M., Desbats, M.A. and Boccaccio, G.L. (2011) RNA granules: the good, the bad and the ugly. Cell. Signal. 23, 324–334.
[5] Decker, C.J. and Parker, R. (2012) P-bodies and stress granules: possible roles in the control of translation and mRNA degradation. Cold Spring Harb. Perspect. Biol. 4, a012286.
[6] Erickson, S.L. and Lykke-Andersen, J. (2011) Cytoplasmic mRNP granules at a glance. J. Cell Sci. 124, 293–297.
[7] Kedersha, N., Stoecklin, G., Ayodele, M., Yacono, P., Lykke-Andersen, J., Fritzler, M.J., Scheuner, D., Kaufman, R.J., Golan, D.E. and Anderson, P. (2005) Stress granules and processing bodies are dynamically linked sites of mRNP remodeling. J. Cell Biol. 169, 871–884.
[8] Tourrière, H., Chebli, K., Zekri, L., Courselaud, B., Blanchard, J.M., Bertrand, E. and Tazi, J. (2003) The RasGAP-associated endoribonuclease G3BP assembles stress granules. J. Cell Biol. 160, 823–831.
[9] Kedersha, N., Cho, M.R., Li, W., Yacono, P.W., Chen, S., Gilks, N., Golan, D.E. and Anderson, P. (2000) Dynamic shuttling of TIA-1 accompanies the recruitment of mRNA to mammalian stress granules. J. Cell Biol. 151, 1257–1268.
[10] Gao, X., Ge, L., Shao, J., Su, C., Zhao, H., Saarikettu, J., Yao, X., Yao, Z., Silvennoinen, O. and Yang, J. (2010) Tudor-SN interacts with and co-localizes with G3BP in stress granules under stress conditions. FEBS Lett. 584, 3525–3532.
[11] Zhu, L., Tatsuke, T., Mon, H., Li, Z., Xu, J., Lee, J.M. and Kusakabe, T. (2013) Characterization of Tudor-sn-containing granules in the silkworm, *Bombyx mori*. Insect Biochem. Mol. Biol. 43, 664–674.
[12] Weissbach, R. and Scadden, A.D. (2012) Tudor-SN and ADAR1 are components of cytoplasmic stress granules. RNA 18, 462–471.
[13] Shaw, N., Zhao, M., Cheng, C., Xu, H., Saarikettu, J., Li, Y., Da, Y., Yao, Z., Silvennoinen, O., Yang, J., Liu, Z.J., Wang, B.C. and Rao, Z. (2007) The multifunctional human p100 protein 'hooks' methylated ligands. Nat. Struct. Mol. Biol. 14, 779–784.
[14] Li, C.L., Yang, W.Z., Chen, Y.P. and Yuan, H.S. (2008) Structural and functional insights into human p100, a key component linking RNA interference and editing. Nucleic Acids Res. 36, 3579–3589.
[15] Välineva, T., Yang, J., Palovuori, R. and Silvennoinen, O. (2005) The transcriptional co-activator protein p100 recruits histone acetyl transferase activity to STAT6 and mediates interaction between the CREB-binding protein and STAT6. J. Biol. Chem. 280, 14989–14996.
[16] Yang, J., Aittomäki, S., Pesu, M., Carter, K., Saarinen, J., Kalkkinen, N., Kieff, E. and Silvennoinen, O. (2002) Identification of p100 as a coactivator for STAT6 that bridges STAT6 with RNA polymerase II. EMBO J. 21, 4950–4958.
[17] Yang, J., Välineva, T., Hong, J., Bu, T., Yao, Z., Jensen, O.N., Frilander, M.J. and Silvennoinen, O. (2007) Transcriptional co-activator protein p100 interacts with snRNP proteins and facilitates the assembly of the spliceosome. Nucleic Acids Res. 35, 4485–4494.
[18] Gao, X., Zhao, X., Zhu, Y., He, J., Shao, J., Su, C., Zhang, Y., Zhang, W., Saarikettu, J., Silvennoinen, O., Yao, Z. and Yang, J. (2012) Tudor staphylococcal nuclease (Tudor-SN) participates in small ribonucleoprotein (snRNP) assembly via interacting with symmetrically dimethylated Sm proteins. J. Biol. Chem. 287, 18130–18141.
[19] Paukku, K., Kalkkinen, N., Silvennoinen, O., Kontula, K.K. and Lehtonen, J.Y. (2008) P100 increases AT1R expression through interaction with AT1R 3′-UTR. Nucleic Acids Res. 36, 4474–4487.
[20] Phetrungnapha, A., Panyim, S. and Ongvarrasopone, C. (2013) Penaeus monodon Tudor staphylococcal nuclease preferentially interacts with N-terminal domain of Argonaute-1. Fish Shellfish Immunol. 34, 875–884.
[21] Sakamoto, K., Yamasaki, Y., Kaneto, H., Fujitani, Y., Matsuoka, T., Yoshioka, R., Tagawa, T., Matsuhisa, M., Kajimoto, Y. and Hori, M. (1999) Identification of oxidative stress-regulated genes in rat aortic smooth muscle cells by suppression subtractive hybridization. FEBS Lett. 461, 47–51.
[22] Wang, Z., Ni, J., Shao, D., Liu, J., Shen, Y., Zhou, L., Huang, Y., Yu, C., Wang, J., Xue, H. and Lu, L. (2013) Elevated transcriptional co-activator p102 mediates angiotensin II type 1 receptor up-regulation and extracellular matrix overproduction in the high glucose-treated rat glomerular mesangial cells and isolated glomeruli. Eur. J. Pharmacol. 702, 208–217.
[23] Dit Frey, N.F., Muller, P., Jammes, F., Kizis, D., Leung, J., Perrot-Rechenmann, C. and Bianchi, M.W. (2010) The RNA binding protein Tudor-SN is essential for stress tolerance and stabilizes levels of stress-responsive mRNAs encoding secreted proteins in Arabidopsis. Plant Cell. 22, 1575–1591.
[24] Sami-Subbu, R., Choi, S.B., Wu, Y., Wang, C. and Okita, T.W. (2001) Identification of a cytoskeleton-associated 120 kDa RNA-binding protein in developing rice seeds. Plant Mol. Biol. 46, 79–88.
[25] Wang, C., Washida, H., Crofts, A.J., Hamada, S., Katsube-Tanaka, T., Kim, D., Choi, S.B., Modi, M., Singh, S. and Okita, T.W. (2008) The cytoplasmic-localized, cytoskeletal-associated RNA binding protein OsTudor-SN: evidence for an essential role in storage protein RNA transport and localization. Plant J. 55, 443–454.
[26] Lei, Y., Huang, Y., Zhang, H., Yu, L., Zhang, M. and Dayton, A. (2011) Functional interaction between cellular p100 and the dengue virus 3′ UTR. J. Gen. Virol. 92, 796–806.
[27] Ascano, M., Hafner, M., Cekan, P., Gerstberger, S. and Tuschl, T. (2012) Identification of RNA-protein interaction networks using PAR-CLIP. Wiley Interdiscip. Rev. RNA 3, 159–177.
[28] Miura, S., Saku, K. and Karnik, S.S. (2003) Molecular analysis of the structure and function of the angiotensin II type 1 receptor. Hypertens. Res. 26, 937–943.
[29] Miura, S., Imaizumi, S. and Saku, K. (2013) Recent progress in molecular mechanisms of angiotensin II type 1 and 2 receptors. Curr. Pharm. Des. 19, 2981–2987.

[30] Mueller, C.F., Wassmann, K., Berger, A., Holz, S., Wassmann, S. and Nickenig, G. (2008) Differential phosphorylation of calreticulin affects AT1 receptor mRNA stability in VSMC. Biochem. Biophys. Res. Commun. 370, 669–674.
[31] Backlund, M., Paukku, K., Daviet, L., De Boer, R.A., Valo, E., Hautaniemi, S., Kalkkinen, N., Ehsan, A., Kontula, K.K. and Lehtonen, J.Y. (2009) Posttranscriptional regulation of angiotensin II type 1 receptor expression by glyceraldehydes 3-phosphatedehydrogenase. Nucleic Acids Res. 37, 2346–2358.
[32] Pende, A., Giacche, M., Castigliola, L., Contini, L., Passerone, G., Patrone, M., Port, J.D. and Lotti, G. (1999) Characterization of the binding of the RNA-binding protein AUF1 to the human AT(1) receptor mRNA. Biochem. Biophys. Res. Commun. 266, 609–614.
[33] Pende, A., Contini, L., Sallo, R., Passalacqua, M., Tanveer, R., Port, J.D. and Lotti, G. (2008) Characterization of RNA-binding proteins possibly involved in modulating human AT 1 receptor mRNA stability. Cell Biochem. Funct. 26, 493–501.
[34] Paukku, K., Backlund, M., De Boer, R.A., Kalkkinen, N., Kontula, K.K. and Lehtonen, J.Y. (2012) Regulation of AT1R expression through HuR by insulin. Nucleic Acids Res. 40, 5250–5261.
[35] Wang, Y., Zhang, H., Chen, Y., Sun, Y., Yang, F., Yu, W., Liang, J., Sun, L., Yang, X., Shi, L., Li, R., Li, Y., Zhang, Y., Li, Q., Yi, X. and Shang, Y. (2009) LSD1 is a subunit of the NuRD complex and targets the metastasis programs in breast cancer. Cell 138, 660–672.
[36] Querido, E. and Chartrand, P. (2008) Using fluorescent proteins to study mRNA trafficking in living cells. Methods Cell Biol. 85, 273–392.
[37] Anderson, P. and Kedersha, N. (2008) Stress granules: the Tao of RNA triage. Trends Biochem. Sci. 33, 141–150.
[38] Leung, A.K., Calabrese, J.M. and Sharp, P.A. (2006) Quantitative analysis of Argonaute protein reveals microRNA-dependent localization to stress granules. Proc. Natl. Acad. Sci. USA 103, 18125–18130.
[39] Shav-Tal, Y., Darzacq, X., Shenoy, S.M., Fusco, D., Janicki, S.M., Spector, D.L. and Singer, R.H. (2004) Dynamics of single mRNPs in nuclei of living cells. Science 304, 1797–1800.
[40] Shyu, A.B., Wilkinson, M.F. and van Hoof, A. (2008) Messenger RNA regulation: to translate or to degrade. EMBO J. 27, 471–481.
[41] Caudy, A.A., Ketting, R.F., Hammond, S.M., Denli, A.M., Bathoorn, A.M., Tops, B.B., Silva, J.M., Myers, M.M., Hannon, G.J. and Plasterk, R.H. (2003) A micrococcal nuclease homologue in RNAi effector complexes. Nature 25, 411–414.
[42] David, P.S., Tanveer, R. and Port, J.D. (2007) FRET-detectable interactions between the ARE binding proteins, HuR and p37AUF1. RNA 13, 1453–1468.
[43] Carpio, M.A., López Sambrooks, C., Durand, E.S. and Hallak, M.E. (2010) The arginylation-dependent association of calreticulin with stress granules is regulated by calcium. Biochem. J. 429, 63–72.
[44] Balagopal, V. and Parker, R. (2009) Polysomes, P bodies and stress granules: states and fates of eukaryotic mRNAs. Curr. Opin. Cell Biol. 21, 403–408.
[45] Grande, M.T., Pascual, G., Riolobos, A.S., Clemente-Lorenzo, M., Bardaji, B., Barreiro, L., Tornavaca, O., Meseguer, A. and Lopez-Novoa, J.M. (2011) Increased oxidative stress, the renin–angiotensin system, and sympathetic overactivation induce hypertension in kidney androgen-regulated protein transgenic mice. Free Radic. Biol. Med. 51, 1831–1841.
[46] Varagic, J., Ahmad, S., Nagata, S. and Ferrario, C.M. (2014) ACE2: angiotensin II/angiotensin-(1-7) balance in cardiac and renal injury. Curr. Hypertens. Rep. 16, 420.
[47] Duan, Z., Zhao, X., Fu, X., Su, C., Xin, L., Saarikettu, J., Yang, X., Yao, Z., Silvennoinen, O., Wei, M. and Yang, J. (2014) Tudor-SN, a novel coactivator of peroxisome proliferator-activated receptor γ protein, is essential for adipogenesis. J. Biol. Chem. 289, 8364–8374.